Landform Analysis 42: 25–36
doi: 10.12657/landfana-042-002
Received: 2023.08.04; Accepted: 2023.10.26

Impact of rainfall intensity on soil erosion based on experimental research

Mikołaj Majewski [1], Aleksandra Czuchaj [2], Marek Marciniak [2]

[1] Institute of Geoecology and Geoinformation, Adam Mickiewicz University in Poznań, Poland, mikolaj.majewski@amu.edu.pl
[2] Institute of Physical Geography and Environmental Planning, Adam Mickiewicz University in Poznań, Poland

Abstract: Soil erosion by water is influenced by a major morphogenetic factor – precipitation. Surface runoff, initiated by rainfall, plays a key role in this process. This article addresses the effects of rainfall intensity and soil moisture on soil erosion through a series of rainfall simulations of different intensity and duration. The implementation of measurements at a research station located in the Różany Stream catchment in Poznań made it possible to study the entire water balance within the slope, including precipitation, evaporation, surface runoff and infiltration.
The study included various rainfall intensities, with a focus on extreme events reflecting ongoing climate change and increasing anthropopressure. Rainfall simulations were conducted on both dry and wet ground. The results showed that increasing rainfall intensity led to greater surface runoff and soil loss. Moreover, soil moisture was identified as a critical factor affecting soil erosion, with wetter conditions reducing soil loss while increasing surface runoff.

Key words: surface runoff, soil erosion, field experiment, rainfall simulator, water balance

Introduction

Processes of soil erosion by water occurring widely on inclined surfaces, depending on the intensity of the main morphogenetic factor, namely atmospheric precipitation, can take various dimensions. Soil erosion by water is most often initiated by surface runoff. According to Horton's infiltration theory (1945), surface runoff represents the difference between the amount of water coming from rainfall and the water infiltrating into the substrate, depending on the rate of infiltration. Water flowing down the slope erodes loose material, shaping hillslopes (De Ploey et al. 1976). Many factors influence the magnitude and intensity of soil erosion processes. Key factors include the intensity of rainfall and snowmelt, soil erodibility, slope length and gradient, type of land use and land management practices (Wischmeier, Smith 1978, Renard 1997).

In the context of observed climate change and increasing anthropogenic pressures, the frequency of extreme events, both meteorological, hydrological, and geomorphological, is increasing (Kostrzewski 2001, Kundzewicz, Jania 2007). Extreme events often have a local character, making their registration difficult due to the sparse network of precipitation stations. Despite their impact on a small area, results of these events can be significant.

Rainfalls with high intensity and duration, capable of causing extreme soil erosion events, occur with varying frequency. In regions where such rainfall events are infrequent, simulated rainfall can be used as an alternative to natural rainfall (Iserloh et al. 2013). Rainfall simulators are valuable tools that allow the recognition of soil erosion and surface runoff processes under controlled and reproducible conditions (Iserloh et al. 2013, Boulange et al. 2019). These simulators aim to replicate natural rainfall under controlled laboratory or field conditions, enabling observation and measurement of rainfall effects on different terrain surfaces (Bowyer-Bower, Burt 1989, Sangüesa et al. 2010).

In soil erosion studies, various types of rainfall simulators are used, differing in construction, scale, and complexity, depending on research objectives and available resources. The most popular are small-scale simulators, used in laboratories (Bryan 1974, Mhaske et al. 2019, Fernández-Raga et al. 2022) and as portable field rainfall simulators (Tossell et al. 1987, Humphry et al. 2002, Nowocień et al. 2004, Iserloh et al. 2013). Rainfall simulations on larger areas is costlier and more time-consuming but provides more representative results (Mayerhofer et al. 2017). This is typically achieved using fixed installations in the field, consisting of multiple rainfall nozzles and automated systems for continuous or intermittent rainfall simulations. These simulators use hydraulic systems to generate rainfall by pumping water through a series of nozzles or sprinklers. The intensity and distribution of rainfall can be adjusted based on the system's design (Panini et al. 1997, Elhakeem, Papanicolaou 2009, Majewski 2014, 2020, Mayerhofer et al. 2017, Naves et al. 2020). Designing rainfall simulators for larger areas increases the complexity of the control system, requiring a larger number of sprinklers and resulting in a more intricate simulation process (Nielsen et al. 2019). The choice of rainfall simulator depends on research objectives, study scale, available resources, and the level of control required for accurate reproduction of specific rainfall events.

The aim of the research was to determine runoff and soil losses from the test plot with black fallow under simulated rainfall conditions. This objective was achieved through a series of field experiments involving the large-plot simulation of rainfall with specific characteristics. The experiments allowed for the determining of all components of the water balance within the slope: rainfall, evaporation, surface runoff, and infiltration. Field experiments were conducted at a specially designed research station using the infrastructure of the Poznań-Morasko Integrated Monitoring of Natural Environmental Base Station.

Study area

Surface runoff and soil loss measurements were carried out at a specially designed research station on a selected hillslope within the Różany Stream catchment (52°27'44.1"N, 16°56'27.9"E). This is a small watercourse in the northern part of the Poznań urban agglomeration, with a length of approximately 7 km, which flows into the Warta River. The test plot was located at an elevation ranging from 83 to 85 m a.s.l. on a south-facing slope with an inclination of approximately 6°.

The Różany Stream catchments characterized by significant elevation differences, ranging from 154 m

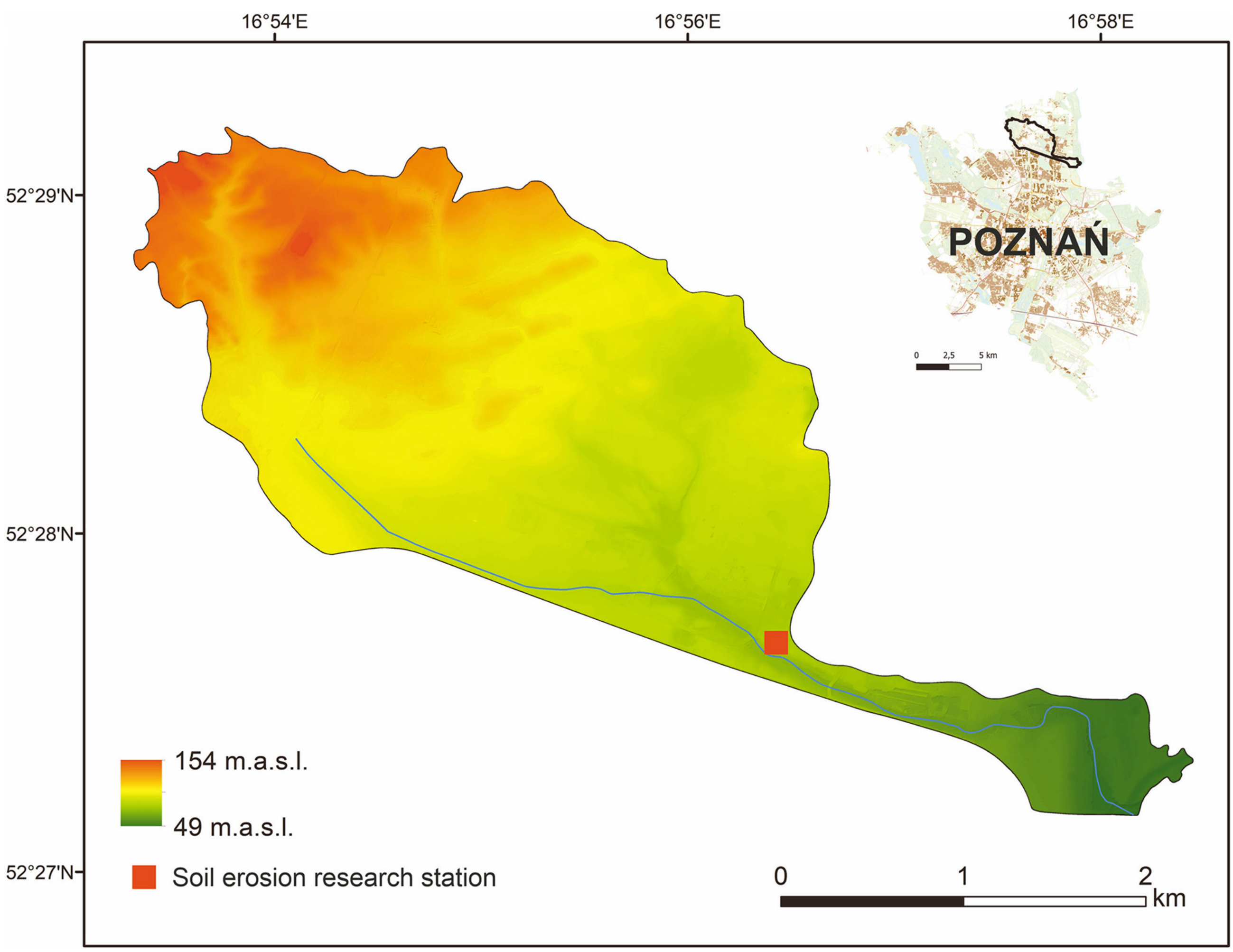

Fig. 1. Location of research station in the Różany Strumień catchment in Poznań, Poland

a.s.l. (Góra Moraska, the highest point in Poznań) to 49 m a.s.l. (mouth of the Różany Stream into the Warta River) (Fig. 1). The average slope inclination in the catchment is approximately 3.8°, which is higher than the average slope inclination of the entire city of Poznań (approximately 3.3°). The range of inclinations that includes the slope with the measurement station (5–8°) covers 13.5% of the catchment area and 8.8% of the area of Poznań. The catchment is characterized by diverse land use. The dominant forms of land use are grass vegetation (33.5%) and forests and wooded areas (26.5%). Arable lands, which are most relevant in terms of soil erosion by water processes, occupy 18.5% of the area. The representativeness of the research station is emphasized by the fact that over 11% of the arable land in the catchment is located on slopes with an inclination in the range of 5–8°.

The activity of the Pleistocene ice sheet influenced the varied topography and lithology in the northern part of Poznań, including the Różany Stream catchment. The landform here takes the form of an undulating moraine plateau, and the most characteristic landforms include accumulative moraine hills (Góra Moraska) and outwash plains (known as the Naramowicki Sandur) (Hildebrandt-Radke 2016, Zwoliński et al. 2017). Among the surface deposits, the largest areas are occupied by glacial till, sands, and gravels (Chmal 1990). In terms of soils, brown soils and rusty soils dominate.

The soil erosion by water research station is located in the immediate vicinity of the building of the Faculty of Geographical and Geological Sciences of Adam Mickiewicz University. The advantage of this location is the shelter provided by the surrounding vegetation, which limits disturbances caused by wind gusts during experiments with simulating rainfall (Czuchaj et al. 2022).

The slope on which the research was conducted is within the area of the Naramowice Sandur's accumulative plain, formed during the Poznań phase of the Weichselian glaciation, in the immediate vicinity of the Różany Stream channel (30 meters away). The slope is characterized by the presence of typical rusty soil, where podzolization processes occur. The soil profile is characterized by a high content of medium and very fine sand. The high content of medium sand characterizes the subsurface level (Ap horizon) as well as deeper horizons, including the bedrock level. On the other hand, a significant amount of very fine and fine sand can be observed in the upper layers of the profile up to a depth of 62 cm. The genetic C horizon shows a noticeable presence of very coarse and coarse sand, accounting for 33% (Major 2018). Soil erodibility index K (Renard et al. 1997) equaled 0.0027. The texture of the surface soil layer is shown in Table 1.

Methods

Testing plot

The soil erosion research station in the Różany Stream catchment consists of 4 plots, each measuring 20 meters in length and 1 meter in width. These plots have different land cover types: black fallow, grass, concrete paver blocks, and asphalt (Fig. 2). In this paper, data from two treatments were used: black fallow and asphalt. The measurements on the asphalt surface were reference only for calculating evaporation and water balance.

Each test plot is bordered by concrete edges that have been sealed at the edges. At the lower part of the test plots, calibrated surface runoff collectors in the form of cylindrical containers with a volume of 300 dm^3 are placed (Fig. 3) (Czuchaj et al., 2022).

The research station allows for monitoring natural rainfall events and conducting experimental research using a rainfall simulator. In July 2022, a series of field experiments were conducted involving artificial rainfall. The rainfall simulation system was designed by a specialized external company, ensuring an 80% uniform rainfall distribution at the testing plot and the implementation of the experimental program.

The hydraulic system for rainfall simulation (Fig. 4) consists of the following devices: a municipal water supply hydrant (1), fire hoses (2) supplying water to a 10 m^3 capacity tank (3), a press pipeline (4), a pumping system (5), a pipeline (6), a collector (7), and a set of nozzles (8) on poles. Depending on the experiment's program, 2 to 8 m^3 of water were required, which was stored in the tank (3). From the tank (3), the water flows through the suction pipeline (4) to the pumping system (5) and then through the press pipeline (6) and the collector (7) to the nozzles (8). The pumping system (5) consists of a pump, a time controller, fuses, a filter, and a flow meter, which allows for pressure and instantaneous flow regulation. The nozzle system consists of 18 poles evenly distributed along the outer boundaries of the research site. The poles have different heights to ensure that all nozzles are at the same level, providing uniform water pressure at the outlets of the individual nozzles. Different types and configurations of nozzles (Fig. 5) allowed for the simulation of seven

Table 1. Surface layer soil texture at the test plot

grain size [mm]	>2	2.0–1.0	1.0–0.1	0.1–0.05	0.05–0.02	0.02–0.005	0.005–0.002	<0.002
content of fraction [%]	2	3	81	5	6	1	2	0

Fig. 2. Soil erosion research station

Fig. 3. Surface runoff and soil loss collector

Fig. 5. Nozzle used for rainfall simulation

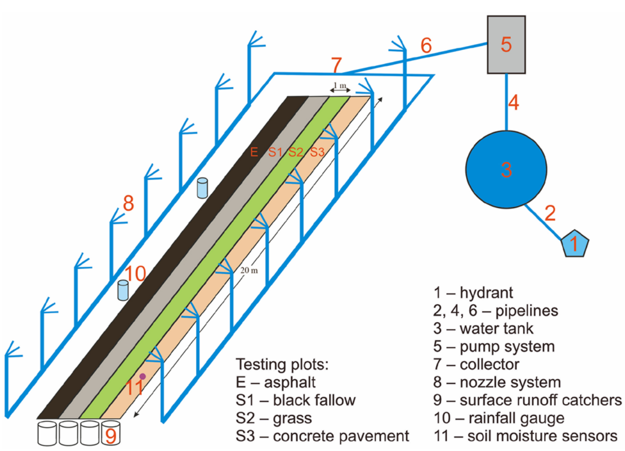

Fig. 4. Schema of the hydraulic system for rainfall simulation

rainfall intensities. To control the programmed rainfall amount, two Hellmann rain gauges were placed on the test plot.

Soil erosion measurements

The volume of surface runoff was determined based on the increase of the water level in the collectors recorded by digital water level sensors (Solinst Levelogger 5 and Solinst Barologger). The water level was recorded at 1-minute intervals. The amount of sediment washed from the black fallow surface was calculated using a weighing method by determining the suspension concentration in a water sample. Water samples with sediment were collected once after each simulation directly from the collector and were filtered in the laboratory of the Poznań-Morasko IMNE Station using Munktells filter papers (84 g·m^{-2}) and then dried at 105°C. After drying, the weight of the collected material was measured with an accuracy of 0.0001 g. Finally, knowing the sample volume and the total surface runoff volume, the total mass of material accumulated in the collector was calculated.

Water balance

The water balance equation for the water cycle on the slope can be simplified as follows:

$$P = E + H_P + I$$

where:
- P – precipitation (rainfall),
- E – evaporation,
- H_P – surface runoff,
- I – infiltration.

The asphalt surface is impermeable, which allowed for the estimation of water evaporation from the flowing water down the slope.

Evaporation during an experiment with simulated rainfall is difficult to estimate. The evaporation process can be divided into two stages: evaporation during the path of water droplets from the simulator nozzles to the slope surface, and evaporation during the runoff on slope surfaces with different coverage. In the first stage, evaporation does not depend on the type of coverage of the test plots. In the second stage, the amount of evaporation will be affected by the thermal properties of the different surfaces. Due to the color and heat capacity, the greatest evaporation is expected from an asphalt surface. Evaporation from a surface with different coverage is difficult to estimate, because there are no methods to correct the amount of evaporation due to different land cover. As a guide, evapotranspiration from a grassy surface was estimated using the Penman-Monteith method based on data recorded by a Davis weather station, which was located in close proximity to the test plot. Over the range of simulated precipitation from A0 to B2, evapotranspiration varied from 5.83% to 0.96% of rainfall. In contrast, evaporation from the asphalt surface ranged from 29.0% to 50.1% of rainfall (Table 2). It can be seen that the amount of evaporation is determined by the first stage of this process during the path of water droplets from the simulator nozzles to the slope surfaces. In view of the impossibility of accurate taking into account the effect of varying land cover on the amount of evaporation, evaporation from the asphalt surface was taken as an estimate of evaporation on the other surfaces. Knowing the total rainfall, evaporation, and surface runoff, the infiltration can be calculated. Additionally, four automatic soil moisture sensors (MEC10 Soil Moisture & Temperature & EC Sensor) were installed at depths of 5, 10, 20, and 50 cm below ground level.

The program of experiments with simulated rainfall

The experimental research program was developed using Chomicz's (1951) rainfall classification widely used in the Polish literature, which reflects well the different types of rainfall, from ordinary to heavy to torrential. The classification categorizes rainfall based on the α coefficient, calculated using the formula:

$$\alpha = \frac{P}{t^{\frac{1}{2}}}$$

where:
- P – total rainfall amount [mm],
- t – rainfall duration [min].

Table 2. Evaporation (E) and evapotranspiration (ET) at the asphalt and grass surfaces

Ground conditions	Category	P [mm]	E asphalt [mm]	ET grass [mm]	E asphalt [%]	ET grass [%]
dry	A0	26.4	8.40	1.54	31.82	5.83
	A1	26.5	10.40	1.29	39.25	4.87
	A2	24.9	11.50	0.91	46.18	3.63
	A3	23.6	10.30	0.44	43.64	1.86
	A4	30.3	12.90	0.29	42.57	0.96
	B1	49.5	24.50	0.94	49.49	1.90
	B2	68.0	32.90	0.89	48.38	1.31
wet	A0	26.2	7.60	1.37	29.01	5.23
	A1	25.9	10.50	1.29	40.54	4.98
	A2	24.9	11.80	1.11	47.39	4.44
	A3	23.4	9.40	0.42	40.17	1.79
	A4	30.5	13.20	0.39	43.28	1.28
	B1	49.5	24.00	1.12	48.48	2.26
	B2	67.7	34.30	0.99	50.66	1.46

Table 3. Program of experiment

Date	Time		Ground conditions	Category	Rainfall intensity	Rainfall duration	Rainfall depth
	Start	End			[mm·h⁻¹]	[min]	[mm]
07.07.2022	11:00	17:15	dry	A0	4	360	24
08.07.2022	9:00	15:15	wet	A0	4	360	24
22.07.2022	10:00	13:10	dry	A1	8	180	24
22.07.2022	13:15	16:30	wet	A1	8	180	24
20.07.2022	10:30	12:10	dry	A2	16	90	24
20.07.2022	12:30	14:10	wet	A2	16	90	24
11.07.2022	10:00	11:00	dry	A3	30	50	25
11.07.2022	11:30	12:30	wet	A3	30	50	25
15.07.2022	11:00	11:55	dry	A4	40	45	30
15.07.2022	12:45	13:40	wet	A4	40	45	30
13.07.2022	10:50	12:05	dry	B1	50	60	50
13.07.2022	13:05	14:20	wet	B1	50	60	50
18.07.2022	10:50	12:15	dry	B2	60	70	70
18.07.2022	12:50	14:15	wet	B2	60	70	70

The program of experiments included three types of rainfall with seven different amounts, intensities, and durations: strong rain (category A0), heavy rain (categories: A1, A2, A3, A4), and torrential rain (categories: B1, B2) (Table 3). Each rainfall was simulated twice: under dry ground conditions and wet ground conditions. Dry ground conditions refer to soil that has not been wetted for at least 24 hours before the rainfall. Experiments under wet ground conditions were conducted immediately after the simulations for dry ground conditions. Additionally, a minimum of 2 days was allowed between simulations of different rainfall categories to achieve similar initial soil moisture conditions. The time of the experiment begins with the start of the sprinkler system and ends with the end of surface runoff to the collectors.

Table 4. Weather conditions during the simulated rainfall experiment

Date	Rainfall category	Ground conditions	Temperature	Wind speed
			[°C]	[m·s⁻¹]
07.07.2022	A0	dry	19.6	0.03
08.07.2022	A0	wet	19.7	0.03
22.07.2022	A1	dry	27.3	0.00
22.07.2022	A1	wet	28.9	0.00
20.07.2022	A2	dry	32.8	0.00
20.07.2022	A2	wet	35.0	0.00
11.07.2022	A3	dry	18.7	0.00
11.07.2022	A3	wet	18.6	0.10
15.07.2022	A4	dry	17.3	0.00
15.07.2022	A4	wet	18.6	0.20
13.07.2022	B1	dry	24.7	0.00
13.07.2022	B1	wet	26.0	0.00
18.07.2022	B2	dry	23.9	0.00
18.07.2022	B2	wet	25.9	0.00

For the comparability of the conducted rainfall simulations, similar weather conditions were crucial, which were determined based on measurements from an automatic weather station (DAVIS) located approximately 80 meters away from the test plot. Each simulated rainfall was carried out under sunny, rainless, and nearly windless conditions, with similar air temperatures (Table 4).

Results

Soil moisture

Soil moisture, in combination with rainfall intensity, is a key factor influencing the volume of surface runoff (Fitzjohn et al. 1998). Wet soils may double the runoff coefficient and shorten the time to runoff, compared with the same soils when dry (Li et al. 2011). Therefore, it was crucial to conduct rainfall simulations under similar soil moisture conditions.

The initial soil moisture was lowest during the first simulation, rainfall A0, which had the lowest intensity. It was 13.7% at a depth of 5 cm and decreased with increasing depth (6.2% at 50 cm depth). For the other simulations, soil moisture at 5 cm depth was very similar, ranging from 17.2% to 19.9%. Similar relationships were observed at greater depths: 10 cm, 20 cm, and 50 cm (Fig. 6).

Each rainfall simulation on dry soil resulted in increased soil moisture at shallow depths (5–10 cm). The increase ranged from 3.2 to 8.2% at a depth of 5 cm and from 2.7 to 7.6% at a depth of 10 cm. The largest increases were recorded for rainfall A0. For the remaining simulations, the standard deviation of moisture increase did not exceed 0.95%. At a depth

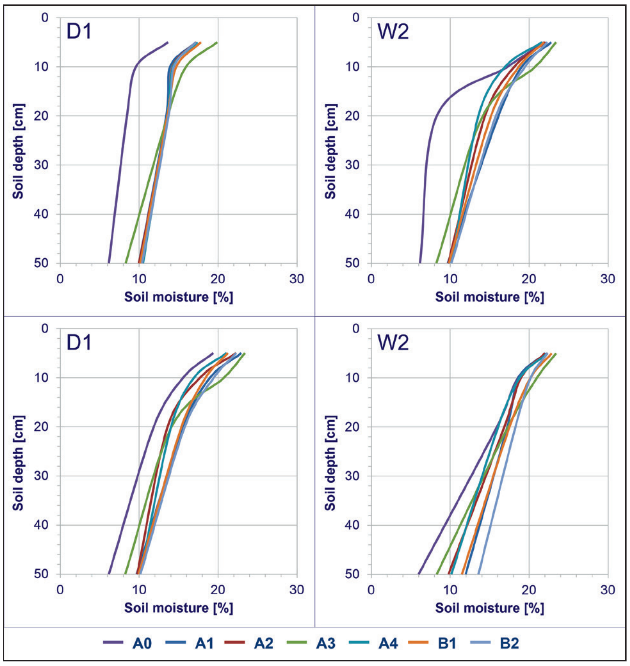

Fig. 6. Initial (1) and final (2) soil moisture in dry (D) and wet (W) conditions

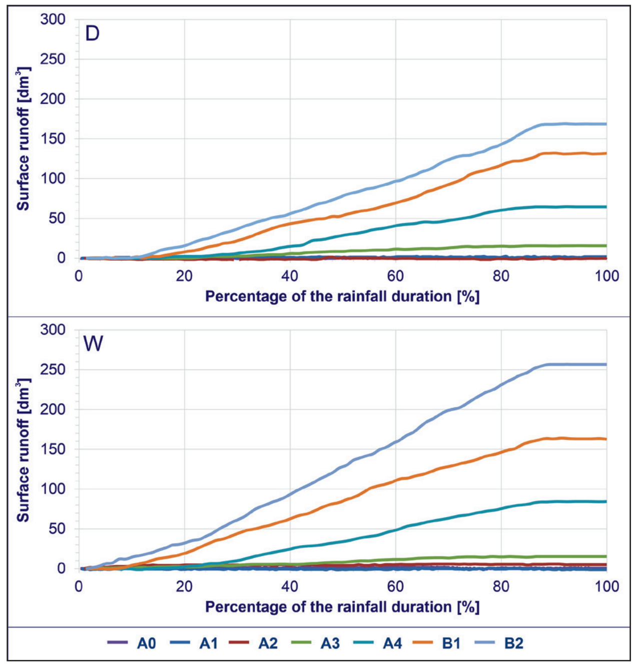

Fig. 7. Dynamic runoff curves for different types of rainfall at black fallow plot in dry (D) and wet (W) conditions

of 20 cm, the increase in moisture was negligible (<1 percentage point) for strong and heavy rains (A0–A4). However, for torrential rains (B1–B2), the moisture increased by 2–3%. No noticeable variation in moisture was observed at a depth of 50 cm.

During simulations on wet soil conditions, the soil moisture resembled the moisture increase during the initial rainfall series, and at a depth of 5 cm, it was higher than the initial moisture by 3.5–5.0%. Rainfall simulations on wet soil did not result in changes in soil moisture shallow layers (5–10 cm), while greater increases (from 1.5 to 3%) were registered at a depth of 20 cm. Double series of rainfall with the highest intensities (B1–B2) also affected the soil moisture increase at a depth of 50 cm (by 3.5–4%).

Surface runoff

Recording surface runoff at a 1-minute time step enabled the analysis of surface runoff dynamics during the individual simulations. Surface runoff is characterized by three values – the initiation moment of runoff, the moment of water level stabilization in the collector, and the slope angle of the curve (Czuchaj et al. 2022).

During the simulations of the lowest intensities (A0–A1), surface runoff did not occur at all on the black fallow plot. Also, for the rainfall event with an intensity of 16 mm·h^{-1} (A2), surface runoff reached very low values, therefore, it was not subjected to detailed analysis.

The initiation of surface runoff, defined as the time when water appeared in the collector, occurred earlier as the rainfall intensity increased. In the case of application of rain on dry soil, runoff started the fastest, in the 8th minute of simulation with a rainfall intensity of 60 mm·h^{-1}. On the other hand, runoff initiation was the latest at an intensity of 30 mm·h^{-1}, occurring in the 17th minute of rainfall. Application of rain on a wet surface generated runoff much earlier, ranging from the 2nd minute (60 mm·h^{-1}) to the 14th minute of rainfall (30 mm·h^{-1}).

From the moment surface runoff began until its end, its increase was relatively uniform for each rainfall event. The rate of surface runoff increased with the intensity of the rainfall. For dry surface, it ranged from 0.3 dm^3·min^{-1} for A3 rainfall, to 2.0 dm^3·min^{-1} for A4 rainfall, 2.5 dm^3·min^{-1} for B1 rainfall, and 2.7 dm^3·min^{-1} for B2 rainfall. As a result of simulation on a wet surface, except for A3 rainfall where the rate was also 0.3, the rate of surface runoff growth was higher for the remaining rainfall events, reaching 2.2 dm^3·min^{-1} for A4 rainfall, 3.0 dm^3·min^{-1} for B1 rainfall, and 3.8 dm^3·min^{-1} for B2 rainfall (Fig. 7).

Water balance

A series of rainfall simulations with different amounts and intensities allowed for the determination of the variability of the simplified water balance (rainfall, evaporation, surface runoff, and infiltration) depending on the rainfall characteristics. The rainfall amount is predefined by the experimental program. Evaporation is calculated based on measurements from an impermeable surface where no infiltration occurs. Surface runoff is determined based

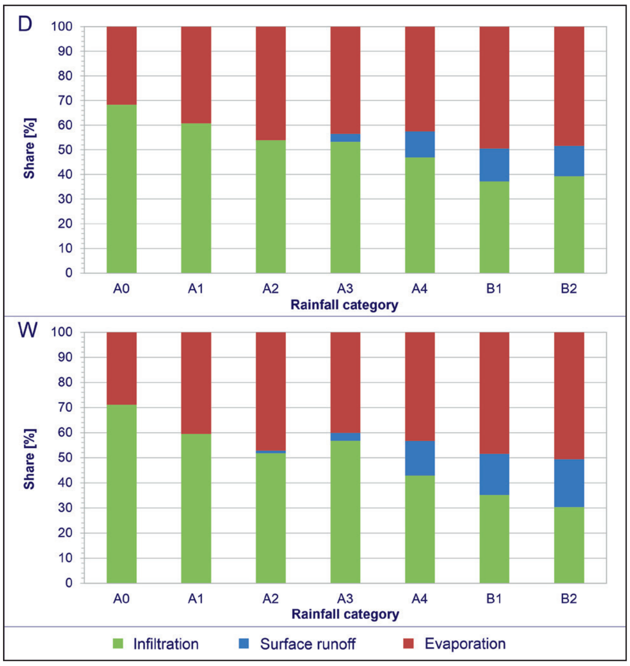

Fig. 8. Water balance for black fallow in different rainfall categories in dry (D) and wet (W) conditions

on loggers installed in the collectors at the bottom of the slope. Infiltration represents the remaining rainfall water that enters the soil.

The share of evaporation in the water balance, regardless of dry or wet soil conditions, increased with the intensity and amount of rainfall. In the case of the weakest simulated rainfall (heavy rain A0), approximately 30% of the rainfall evaporated. However, for torrential rains (B1-B2), evaporation intensified and was accounted for nearly half of the total rainfall amount (Fig. 7).

The surface runoff occurred with the A2 category rainfall and above, so for A0-A1 rainfalls, the remaining portion of the rainfall infiltrated into the soil. The contribution of surface runoff in the water balance, represented by the runoff coefficient (Savenije 1996), increased with both the amount and intensity of rainfall, as well as during simulations under wet conditions. For A2 and A3 rainfall events, the runoff coefficient was low and did not exceed 3.5%. During the highest category heavy rain (A4), the runoff coefficient exceeded 10%. Simulated torrential rains (B1–B2) on dry soil conditions generated surface runoff representing approximately 13% of the total rainfall. The runoff coefficient significantly increased with simulation on a wet soil, reaching a maximum of 19% for the B2 rainfall event (Fig. 8).

Surface runoff and soil erosion

The lack of surface runoff during the least intense rainfall events (A0 and A1) naturally resulted in the lack of the soil loss process. For the remaining rainfall events, both the total amount of surface runoff and soil loss increased with the simulated rainfall intensity. In the case of the A2 rainfall simulation (16 mm·h^{-1} intensity), surface runoff and soil loss only occurred when applicating a rain on a wet surface. The amounts of surface runoff and soil loss for both the A2 and A3 (30 mm·h^{-1}) rainfall events were very small: A2 (<0.001 kg·m^{-2}; ~0.25 dm^3·m^{-2}) and A3 (~0.001 kg·m^{-2}; ~0.75 dm^3·m^{-2}).

Comparing simulations under dry and wet soil conditions, greater soil loss occurred during simulation on the dry surface, while higher surface runoff was observed after simulation on the wet surface. Under wet ground conditions, soil loss accounted from 62% (rainfalls A3, A4) to 92% (rainfall B1) of the soil loss observed under dry conditions. Increased moisture content helps to bind soil particles together, increasing soil stability and reducing particle detachment and transport down the slope. However, it also limits infiltration, resulting in increased surface runoff and reduced soil loss.

For the simulations of the highest intensity rainfall events (A4, B1, B2), the increase in surface runoff followed a linear pattern, while the increase in soil loss exhibited a power function. The total surface runoff during simulation on dry soil ranged from 3.2 dm^3·m^{-2} (A4) to 8.4 dm^3·m^{-2} (B2), and during simulation on wet soil, it ranged from 4.2 dm^3·m^{-2} to 12.8 dm^3·m^{-2}. The soil loss ranged from 0.004 kg·m^{-2} to 0.032 kg·m^{-2} under dry conditions, and from 0.002 kg·m^{-2} to 0.024 kg·m^{-2} under wet conditions (Fig. 9). With each more intense rainfall event, the

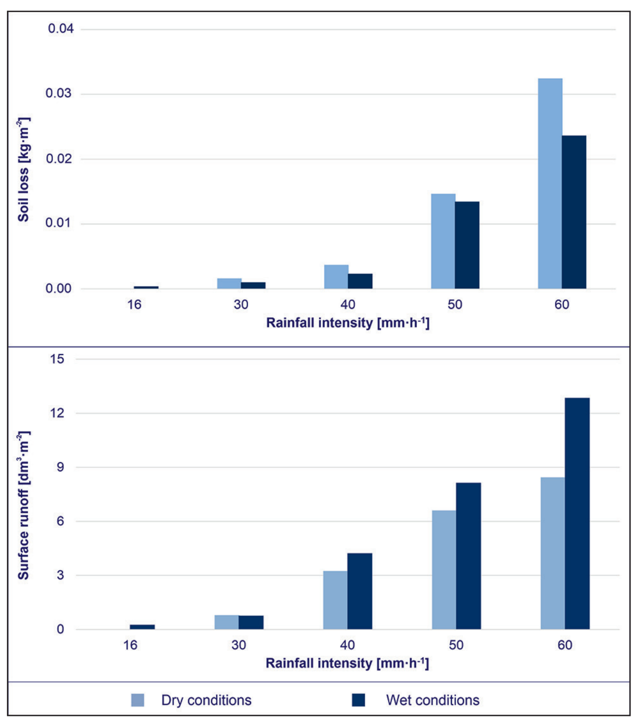

Fig. 9. Soil loss and surface runoff under simulated rainfall with different intensities

suspension concentration in the collectors also increased. For dry conditions, it was 1.13 g·dm^{-3} (A4), 2.22 g·dm^{-3} (B1), and 3.85 g·dm^{-3} (B2), while for wet conditions, it was 0.54 g·dm^{-3} (A4), 1.65 g·dm^{-3} (B1), and 1.84 g·dm^{-3} (B2).

Soil loss during the A2–A4 rainfall events exhibited a interrill character, while during the B1–B2 rainfalls, it initially had a dispersed character but tended to concentrate into water streams, gradually transitioning into linear erosion. Despite the limited length of the surface and, consequently, the smaller amount of water flowing down the slope, rill erosion occurred during the most intense rainfall simulation.

Discussion

With the increasing frequency of extreme rainfall events (Fowler et al. 2021), understanding their impact on soil erosion becomes crucial for effective soil management and conservation practices. Studying soil erosion by water under natural rainfall conditions is very challenging. Waiting for natural rainfall events with varying intensities could take years, and the results would still be uncertain. Therefore, the use of rainfall simulators may enable the study of the erosion effects of rainfall with different intensity, both low and high. Various configurations of nozzles in the rainfall simulator allowed for the replication of different rainfall intensities, enabling the determination of the impact of rainfall intensity on the magnitude of soil erosion.

Simulating natural rainfall is highly complex and may not perfectly replicate the intricacies of natural rainfall in both laboratory and field conditions (Abudi et al. 2012, Rončević et al. 2023). Rainfall simulators in soil erosion by water studies have not yet been standardized. Simulators differ in construction, rainfall intensity, rainfall uniformity, droplet sizes, and droplet velocities, making it difficult to draw meaningful comparisons between results (Iserloh et al. 2013).

One significant issue is the height from which the droplets fall during the simulated rainfall. In previous research most simulations were conducted with a fall height of up to 2 meters (Rončević et al. 2023). Achieving a sufficiently large falling height is even more challenging for application rain on large areas (Majewski 2020). Due to the slope inclination, the nozzles of the rain simulator must be positioned at different heights above the ground to ensure that water outflow occurs at the same hydraulic potential for each nozzle. In this situation, it is not possible to consider the impact of the height of rainfall drops at different locations on the slope. The falling height was consistent during each simulation, ensuring that it does not negatively affect the comparison of the impact of rainfall intensity on surface runoff and soil loss. The height of the rainfall and the size of the raindrops need to be resolved in the standardization process of rainfall simulation

Dunkerley (2021) notes that constant intensity rainfall, which is commonly used in rainfall simulation experiments, neglects both rapid fluctuations in rainfall intensity and intensity profiles occurring in natural conditions. In this study, examining the impact of rainfall with different amounts, durations, and intensities, constant intensities were used during each individual rainfall event. However, further, more detailed research is planned, involving rainfall events with the same amount and duration but varying intensity.

The crucial factor initiating soil loss is water flowing down the slope. Therefore, an essential aspect of the research was to determine the water balance within the slope. In studies of surface runoff, evaporation is often an overlooked component of the water balance (Bettoni et al. 2023), but it plays a significant role, especially during intense rainfall events. With an increase in rainfall intensity, the share of water evaporating from the surface also rises.

During intense rainfall events, the soil quickly becomes saturated, leading to excess water on the surface. This surplus water increases the availability of water for evaporation. Additionally, during heavy rainfall, the air tends to be more humid due to the presence of moisture from the rainfall, providing a greater source of water vapor to the atmosphere.

However, it is essential to emphasize that while intense rainfall can temporarily increase evaporation, the overall impact of rainfall on the water balance of an area depends on various other factors, such as the duration and frequency of rainfall, existing soil moisture, and local climatic conditions. Long-term trends in rainfall and evaporation are influenced by complex interactions between these factors (IPCC 2021).

The annual runoff coefficient calculated from stationary measurements on sandy slopes in the Gniezno Lakeland in the late 1980s was 4.5% (Kosturkiewicz, Szafrański 1993). Similar values were obtained on the surface with clayey sands in the Chwalimski Brook catchment in the Drawskie Lakeland in 1994–1996 (Szpikowski 2003) and 2012–2014 (Majewski 2020). In contrast, on sandy slopes in the Suwalskie Lakeland, surface runoff accounted for 2% of rainfall (Smolska 2010). Runoff coefficients during the experiments were comparable only for the lowest intensity rainfalls (up to 30 mm·h^{-1}). For more intense rainfalls, runoff coefficients already reached several times higher values (11–18%). The A4 category precipitation (intensity: 40 mm·h^{-1}, duration: 45 min, depth: 30 mm) can be compared with the rainfall simulated during field experiments in the Drawsko

Lakeland in 2013–2014, in the catchments of Chwalimski Potok and Kluda (intensity: 38 mm·h^{-1}, duration: 50 min, depth: 32 mm). The runoff coefficient on the slope in the Różany Stream catchment (11%) was lower than that on the sandy slope in the Kluda catchment (15%) and significantly lower than that on the slope with clayey sands in the Chwalimski Brook catchment (38%) (Majewski 2020).

On the other hand, the average annual value of soil loss in the Chwalimski Brook catchment was 0.46 kg·m^{-2} in 1994–1996 (Szpikowski 2003) and 0.37 kg·m^{-2} in 2012–2014 (Majewski 2020). Slightly lower volumes of 2.7 kg·m^{-2} occurred in the Suwalskie Lakeland (Smolska 2010). The maximum soil erosion values during single rainfall events on the slope in the Różany Stream catchment (0.03 kg·m^{-2}) were only about 10% of these values. On the other hand, compared to soil loss under simulated rainfall in the Drawskie Lakeland, the values obtained in Poznań during A4 precipitation (0.004 kg·m^{-2}) were 10 times lower than on the sandy slope in the Kluda catchment (0.04 kg·m^{-2}) and tens of times lower than on the slope with clayey sands in the Chwalimski Brook catchment (0.25 kg·m^{-2}). Higher permeability and lower soil erodibility index in the Różany Stream catchment were important factors for lower surface runoff and soil loss.

Conclusions

The conducted research showed that with an increase in rainfall intensity, the magnitude of surface runoff and soil erosion also increased, but also showed a significant impact of soil moisture on soil erosion. Water-saturated sediments lose their infiltration capacity and become the cause of accelerated surface runoff, leading to a reduction in the soil's infiltration capacity and, consequently, a quicker initiation of surface runoff compared to dry soils (Słupik 1981, Winowski, Majewski 2016). The opposite situation occurred in the case of soil loss, where, with an increase in initial moisture content, soil loss decreased. Similar results were obtained during laboratory simulations by Rudolph et al. (1997) and Brodowski and Rejman (2004). Soil with higher moisture content exhibits greater cohesion, which hinders the detachment and transport of its particles down the slope. However, it is essential to remember that excessive soil saturation can lead to increased slope instability and the possibility of mass movements, such as landslides or mudslides.

The conducted research has enriched the knowledge regarding soil erosion by water processes under simulated rainfall conditions. It has demonstrated the significant impact of soil moisture and rainfall intensity on surface runoff and soil loss. The obtained results emphasize the importance of considering these factors in soil erosion management and conservation efforts. The research has also highlighted the usefulness of rainfall simulators as tools for replicating and evaluating various rainfall scenarios, providing valuable insights into erosion processes under controlled conditions.

With ongoing climate changes leading to more frequent extreme rainfalls, these studies contribute to a better understanding of the threats associated with soil erosion and can aid in the development of effective strategies to mitigate their impact on the natural environment.

Acknowledgments

This research was partially supported by the project: Initiative of Excellence—Research University at Adam Mickiewicz University, Poznan, Poland, grant number 038/04/NP/0006. Special thanks to Ryszard Łukowicz for the design and implementation of the rainfall simulator. We also thank two anonymous reviewers for all valuable comments.

Author's contribution

MMaj, AC, MMar designed and built the test plot, conceptualized and implemented the experiments, MMaj prepared and interpreted the results, MMaj, MMar edited and proofread the text.

References

Abudi I., Carmi G., Berliner P., 2012. Rainfall simulator for field runoff studies. Journal of Hydrology 454: 76–81. DOI: 10.1016/j.jhydrol.2012.05.056.

Bettoni M., Maerker M., Bosino A., Conedera M., Simoncelli L., Vogel S., 2023. Land use effects on surface runoff and soil erosion in a southern Alpine valley. Geoderma 435, 116505. DOI: 10.1016/j.geoderma.2023.116505.

Boulange J., Malhat F., Jaikaew P., Nanko K., Watanabe H., 2019. Portable rainfall simulator for plot-scale investigation of rainfall-runoff, and transport of sediment and pollutants. International journal of sediment research 34(1): 38–47. DOI: 10.1016/j.ijsrc.2018.08.003.

Bowyer-Bower T.A.S., Burt T.P., 1989. Rainfall simulators for investigating soil response to rainfall. Soil Technology 2, 1: 1–16. DOI: 10.1016/S0933-3630(89)80002-9.

Brodowski R., Rejman J., 2004. Określenie wpływu wilgotności i stanu powierzchni gleby wytworzonej z piasku gliniastego na spływ powierzchniowy i zmyw gleby. Acta Agrophysica 4(3): 619–624.

Bryan R.B., 1974. A simulated rainfall test for the prediction of soil erodibility. Zeitschrift fur Geomorphologie N.F. Supplement Band 21: 138–150.

Chmal R., 1990. Szczegółowa Mapa Geologiczna Polski w skali 1:50 000, arkusz Poznań. Warszawa, Państwowy Instytut Geologiczny.

Chomicz K., 1951. Ulewy i deszcze nawalne w Polsce. Wiad. Służby Hydrol. Meteor 2: 5–58.

Czuchaj A., Majewski M., Marciniak M., 2022. Koncepcja stanowiska do badań spływu powierzchniowego i spłukiwania w zlewni Różanego Strumienia. In: A. Kostrzewski, J. Szpikowski, M. Majewski (eds.), Zintegrowany Monitoring Środowiska Przyrodniczego. Współczesne przemiany naturalne i antropogeniczne środowiska przyrodniczego zlewni rzecznych i jeziornych. Bogucki Wydawnictwo Naukowe, Poznań: 163–179.

De Ploey J., Savat J., Moeyersons J., 1976. The differential impact of some soil loss factors on flow, runoff, creep and rainwash. Earth Surface Processes 1: 151–162.

Dunkerley D., 2021. The importance of incorporating rain intensity profiles in rainfall simulation studies of infiltration, runoff production, soil erosion, and related landsurface processes. Journal of Hydrology 603, 126834. DOI: 10.1016/j.jhydrol.2021.126834.

Elhakeem M., Papanicolaou A.N., 2009. Estimation of the Runoff Curve Number via Direct Rainfall Simulator Measurements in the State of Iowa, USA. Water Resources Management 23(12): 2455–2473. DOI: 10.1007/s11269-008-9390-1.

Fernández-Raga M., Rodríguez I., Caldevilla P., Búrdalo G., Ortiz A., Martínez-García R., 2022. Optimization of a Laboratory Rainfall Simulator to Be Representative of Natural Rainfall. Water 14(23), 3831. DOI: 10.3390/w14233831.

Fitzjohn C., Ternan J.L., Williams A.G., 1998. Soil moisture variability in a semi-arid gully catchment: implications for runoff and erosion control. Catena 32(1): 55–70. DOI: 10.1016/S0341-8162(97)00045-3.

Fowler H.J., Lenderink G., Prein A.F., Westra S., Allan R.P., Ban N., Barbero R., Berg P., Blenkinsop S., Do H.X., Guerreiro S., Haerter J.O., Kendon E.J., Lewis E., Schaer C., Sharma A., Villarini G., Wasko C., Zhang X., 2021. Anthropogenic intensification of short-duration rainfall extremes. Nature Reviews Earth & Environment 2(2): 107–122. DOI: 10.1038/s43017-020-00128-6.

Hildebrandt-Radke I., 2016. Środowisko geograficzne Poznania. In: M. Kara, M. Makohonienko, A. Michałowski (eds), Przemiany osadnictwa i środowiska przyrodniczego Poznania i okolic od schyłku starożytności do lokacji miasta. Bogucki Wydawnictwo Naukowe, Poznań: 23–46.

Horton R., 1945. Erosional development of streams and their drainage basins: hydrophysical approach to quantitative morphology. Bulletin of the Geological Society of America 56: 275–370.

Humphry J.B., Daniel T.C., Edwards D.R., Sharpley A.N., 2002. A portable rainfall simulator for plot-scale runoff studies. Applied Engineering in Agriculture 18(2): 199–204. DOI: 10.13031/2013.7789.

IPCC, 2021. Climate Change 2021: The Physical Science Basis. Contribution of Working Group I to the Sixth Assessment Report of the Intergovernmental Panel on Climate Change. V. Masson-Delmotte, P. Zhai, A. Pirani, S.L. Connors, C. Péan, S. Berger, N. Caud, Y. Chen, L. Goldfarb, M.I. Gomis, M. Huang, K. Leitzell, E. Lonnoy, J.B.R. Matthews, T.K. Maycock, T. Waterfield, O. Yelekçi, R. Yu, and B. Zhou (eds.). Cambridge University Press, Cambridge, United Kingdom and New York, NY, USA. DOI: 10.1017/9781009157896.

Iserloh T., Ries J.B., Arnáez J., Boix-Fayos C., Butzen V., Cerdà A., Echeverría M.T., Fernández-Gálvez J., Fister W., Geißler C., Gómez J.A., Gómez-Macpherson H., Kuhn N.J., Lázaro R., León F.J., Martínez-Mena M., Martínez-Murillo M.F., Marzen M., Mingorance M.D., Ortigosa L., Peters P., Regüés D., Ruiz-Sinoga J.D., Scholten T., Seeger M., Solé-Benet A., Wengel R., Wirtz S., 2013. European small portable rainfall simulators: A comparison of rainfall characteristics. Catena 110: 100–112. DOI: 10.1016/j.catena.2013.05.013.

Kostrzewski A., 2001. Stan badań erozji gleb na Pomorzu Zachodnim. Folia Universitatis Agriculturae Stetinensis 217, Agricultura 87: 117–124.

Kosturkiewicz A., Szafrański Cz., 1993. Spływy powierzchniowe i podpowierzchniowe z bogato rzeźbionych terenów. In: A. Kostrzewski (ed.), Geoekosystem obszarów nizinnych, Zeszyty Naukowe IGiPZ PAN 6: 123–130.

Kundzewicz Z., Jania J., 2007. Extreme hydro-meteorological events and their impacts. From the global down to the regional scale. Geographia Polonica 80, 2: 9–23.

Li X.Y., Contreras S., Sole-Benet A., Canton Y., Domingo F., Lazaro R., Lin H., Wesemael B.V., Puigdefabregas J., 2011. Controls of infiltration-runoff processes in Mediterranean karst rangelands in SE Spain. Catena 86: 98–109. DOI: 10.1016/j.catena.2011.03.003.

Majewski M., 2014. Wykorzystanie eksperymentu terenowego w badaniach erozji wodnej gleb w zlewni Chwalimskiego Potoku (Pojezierze Drawskie, górna Parsęta). Prace Geograficzne UJ 138: 57–66.

Majewski M., 2020. Sekularne i ekstremalne procesy erozji wodnej gleb na Pojezierzu Drawskim. Landform Analysis 39.

Major M., 2018. Skład granulometryczny gleb rdzawych w zlewni Różanego Strumienia. In: A. Kostrzewski, A. Stach, M. Majewski (eds), Geneza, litologia i stratygrafia utworów czwartorzędowych, t. VII, IGIG UAM, Poznań: 125–130.

Mayerhofer C., Meißl G., Klebinder K., Kohl B., Markart G., 2017. Comparison of the results of a small-plot and a large-plot rainfall simulator–Effects of land use and land cover on surface runoff in Alpine catchments. Catena 156: 184–196. DOI: 10.1016/j.catena.2017.04.009.

Mhaske S.N., Pathak K., Basak A., 2019. A comprehensive design of rainfall simulator for the assessment of soil erosion in the laboratory. Catena 172: 408–420. DOI: 10.1016/j.catena.2018.08.039.

Naves J., Anta J., Suárez J., Puertas J., 2020. Hydraulic, wash-off and sediment transport experiments in a full-scale urban drainage physical model. Scientific data 7(1), 44. DOI: 10.1038/s41597-020-0384-z.

Nielsen K.T., Moldrup P., Thorndahl S., Nielsen J.E., Duus L.B., Rasmussen S.H., Uggerby M., Rasmussen M.R., 2019. Automated rainfall simulator for variable rainfall on urban green areas. Hydrological Processes 33(26): 3364–3377. DOI: 10.1002/hyp.13563.

Nowocień E., Podolski B., Wawer R., 2004. Estimating outflow and sediment uptake chosen Polish soil kinds in simulated conditions. Electronic Journal of Polish Agricultural Universities 7(2).

Panini T., Torri D., Pellegrini S., Pagliai M., Salvador Sanchis M.P., 1997. A theoretical approach to soil porosity and sealing development using simulated rainstorms. Catena 31: 199–218. DOI: 10.1016/S0341-8162(97)00039-8.

Renard K.G., Foster G.R., Weesies G.A, McCool D.K. Yder D.C., 1997. Predicting Soil Erosion by Water: A Guide to Conservation Planning with the Revised Universal Soil Loss Equation (RUSLE) (Agricultural Handbook 703). US Department of Agriculture, Washington DC.

Rončević V., Živanović N., van Boxel J.H., Iserloh T., Štrbac S., 2023. Dripping Rainfall Simulators for Soil Research – Performance Review. Water 15(7), 1314. DOI: 10.3390/w15071314.

Rudolph A., Helming K., Diestel H., 1997. Effect of antecedent soil water content and rainfall regime on microrelief changes. Soil Technology 10: 69–81. DOI: 10.1016/0933-3630(95)00040-2.

Sangüesa C., Arumí J., Pizarro R., Link O., 2010. A Rainfall Simulator for the in situ Study of Superficial Runoff and Soil Erosion. Chilean journal of agricultural research: 178–182.

Savenije H.H., 1996. The runoff coefficient as the key to moisture recycling. Journal of Hydrology 176(1–4): 219–225. DOI: 10.1016/0022-1694(95)02776-9.

Słupik J., 1981. Rola stoku w kształtowaniu odpływu w Karpatach fliszowych. Prace Geograficzne IGiPZ PAN 142, Kraków.

Smolska E., 2010. Spływ wody i erozja gleby na piaszczystym stoku w obszarze młodoglacjalnym – pomiary poletkowe (Pojezierze Suwalskie, Polska NE). In: E. Smolska, J. Rodzik (eds.), Procesy erozyjne na stokach użytkowanych rolniczo (metody badań, dynamika i skutki). Prace i Studia Geograficzne 45: 197–214.

Szpikowski J., 2003. Contemporary processes of soil erosion and the transformation of the morphology of slopes in agricultural use in the postglacial catchment of the Chwalimski Potok (Up-

per Parsęta, Drawskie Lakeland). Quaestiones Geographicae 22: 79–90.
Tossell R.W., Dickinson W.T., Rudra R.P., Wall G.J, 1987. A portable rainfall simulator. Canadian Agricultural Engineering 29: 155–162.
Winowski M., Majewski M., 2016. Lithological conditions of soil erosion in the Chwalimski Potok catchment (the Drawskie Lakeland) at the background of selected geotechnical analyses. Prace Geograficzne 147: 7–23. DOI: 10.4467/20833113PG.16.019.6081.
Wischmeier W.H., Smith D.D., 1978. Predicting rainfall erosion losses: A guide to conservation planning. Agricultural Handbook 537, U.S. Department of Agriculture, Washington D.C.
Zwoliński Z., Hildebrandt-Radke I., Mazurek M., Makohonienko M., 2017. Existing and proposed urban geosites values resulting from geodiversity of Poznań City. Quaestiones Geographicae 36(3): 125–149. DOI: 10.1515/quageo-2017-0031.